EXPERIMENTAL CELL RESEARCH 316 (2010) 2061–2070

available at www.sciencedirect.com

ScienceDirect

www.elsevier.com/locate/yexcr

Research Article

Upregulation of the GRIM-19 gene suppresses invasion and metastasis of human gastric cancer SGC-7901 cell line

Yi Huang[a,b,*], *MeiHua Yang*[c], *Huaan Yang*[d], *ZhaoChun Zeng*[b]

[a] *Center for Clinical Molecular Medicine, Children's Hospital, Chongqing Medical University, Chongqing 400014, People's Republic of China*
[b] *Department of Biochemistry and Molecular Biology, Chongqing Medical University, Chongqing 400016, People's Republic of China*
[c] *Department of Neurosurgery, Xinqiao Hospital, Third Military Medical University, Chongqing 400037, People's Republic of China*
[d] *Department of Urologic Surgery, Yubei People's Hospital, Chongqing 401120, People's Republic of China*

ARTICLE INFORMATION

Article Chronology:
Received 22 October 2009
Revised version received 7 May 2010
Accepted 8 May 2010
Available online 15 May 2010

Keywords:
GRIM-19
GW112
Gastric cancer
Metastasis
Invasion
NF-κB

ABSTRACT

Gene associated with retinoid-IFN-induced mortality 19 (GRIM-19), as a novel IFN-β/RA-inducible gene product, was identified as a potential tumor suppressor associated with growth inhibition and cell apoptosis. Recently, it has been reported that the apoptotic effects and apoptosis-related gene induction of GRIM-19 can be attenuated by GW112, indicating that GRIM-19 and GW112 are involved in a common signal transduction pathway. To investigate the signaling mechanisms that link GRIM-19 to GW112 and their functional role in tumor cell invasion and metastasis, we utilized adenovirus-mediated overexpression of GRIM-19 in the gastric cancer SGC-7901 cell line. We observed that enhanced expression of GRIM-19 not only downregulated GW112 but also decreased NF-κB binding activity. As a result, we found that tumor cell adhesion, migration, invasion and liver metastasis were inhibited. Additionally, upregulation of GRIM-19 also suppressed secretion of urokinase-type plasminogen activator (u-PA), matrix metalloproteinase (MMP)-2, 9 and vascular endothelial growth factor (VEGF). These results indicate that GRIM-19 acts as an upstream regulator of GW112 to block NF-κB binding activity, thereby inhibiting gastric cancer cell migration, invasion and metastasis. We conclude that adenoviral transfer of the GRIM-19 gene may be an efficacious approach to controlling the invasion and metastasis of human gastric cancer.

Introduction

The combination of IFN-β and all-trans retinoic acid (RA) has been shown to synergistically inhibit tumor activity in a number of animal models and in clinical studies [1,2]. GRIM-19 (gene associated with retinoid-IFN-induced mortality 19), an IFN/RA-inducible gene product, was recently identified as a potential tumor suppressor that promotes IFN/RA-induced cell death [3]. In human breast, prostate and renal carcinoma cells, overexpression of GRIM-19 induces apoptosis, and this is augmented by IFN/RA treatment [4–6]. Moreover, GRIM-19 has been shown to be an inhibitor of signal transducer and activator of transcription 3 (STAT3) by repressing its transcrip-

* *Corresponding author.* Current address: Center for Clinical Molecular Medicine, Children's Hospital of Chongqing Medical University, No.136 Zhongshan Er Road, Yuzhong District, Chongqing, 400014, People's Republic of China. Fax: +86 23 63622866.
E-mail address: yihuang828@yahoo.com.cn (Y. Huang).

Abbreviations: GRIM-19, gene associated with retinoid-IFN-induced mortality 19; ECL, enhanced chemiluminescence; EMSA, electrophoretic mobility shift assay; ELISA, enzyme-linked immunospecific assay; GFP, green fluorescent protein; IF, immunofluorescence; IFN, interferon; MMP, matrix metalloproteinase; PBS, phosphate-buffered saline; u-PA, urokinase-type plasminogen activator; VEGF, vascular endothelial growth factor; WT, wild-type

0014-4827/$ – see front matter © 2010 Elsevier Inc. All rights reserved.
doi:10.1016/j.yexcr.2010.05.010

tional activation [7,8]. Collectively, these observations indicate a potential tumor suppressor-like function for GRIM-19 [9]. Furthermore, the pro-apoptotic effects of GRIM-19 are also inhibited by certain DNA viral oncoproteins such as vIRF1, human papillomavirus-E6, SV40 T antigen [10] and other molecules, including GW112 [11].

GW112, also named OLFM4, is a secreted glycoprotein [12] originally described as human granulocyte colony-stimulating factor stimulated clone-1 (hGC-1) [13]. The importance of GW112 for tumor growth has only recently been appreciated as a result of its overexpression in gastric cancers and its anti-apoptotic effects against GRIM-19 [11–19]. GW112 is frequently overexpressed in many types of human tumors [11,14], including gastric cancer [11,15–18], and it was believed to play a crucial role in the development and progression of gastric carcinogenesis [14–18]. GW112 functionally attenuates the ability of GRIM-19 to mediate retinoic acid-IFN-β-mediated cell apoptosis and apoptosis-related gene expression through its interaction with GRIM-19, indicating that common signal transduction pathways may potentially and functionally link GW112 and GRIM-19 [11]. Although previous studies have shown the strong inhibitory impact of GRIM-19 on the STAT3 transcriptional activity in tumor cells and the involvement of nuclear factor kappa-B (NF-κB) in GW112 expression. However, the potential link between GRIM-19 and GW112 and their regulation of signaling activities contributing towards the malignant phenotype of gastric cancer remain poorly understood.

In this study, we applied adenovirus-mediated GRIM-19 expression (Ad-GRIM-19) to facilitate gene transfer with high-efficiency and lower cytotoxicity toward human gastric cancer SGC-7901 cells. We demonstrate that upregulation of GRIM-19 suppresses the expression of GW112 and decreases NF-κB binding activity. GRIM-19 is also shown to inhibit tumor cell migration and invasion *in vitro* and metastasis *in vivo*. This work is the first to identify a suppressive effect of GRIM-19 on NF-κB binding activity and metastasis in gastric cancer and to establish an "oncogene-tumor suppressor-like" relationship between GRIM-19 and GW112.

Materials and methods

Plasmids and antibodies

The AdEasy system of adenoviral packaging, including the pAdtrack-CMV shuttle vector containing the green fluorescent protein (GFP) report gene, pAdeasy-1 and the packaging *E. coli* BJ5183 cells was kindly provided by Dr. Tong-Chuan He, Johns Hopkins Tumor Center, USA, and preserved by the Department of Biochemistry and Molecular Biology, Chongqing Medical University. All chemicals were purchased from Sigma-Aldrich (St. Louis, MO) unless otherwise specified. Antibodies specific for GRIM-19 (BD Biosciences, San Diego, CA, USA), GW112 (OLFM4) (Abcam, Cambridge, UK), u-PA, MMP-2, MMP-9, β-actin (Santa Cruz, CA, USA), NF-κB p65/RelA, STAT3 and Histone H3 (Santa Cruz, CA, USA) were used in these studies. All secondary antibodies were purchased from Santa Cruz Biotechnology, Inc.

Cell lines and cell culture

The human gastric carcinoma metastatic lymph node cell line SGC-7901 and low-passage human embryonic kidney 293T cells (HEK-293T) were purchased from CBTCCCAS (the Cell Bank of Type Culture Collection of Chinese Academy of Sciences, Shanghai Institute of Cell Biology, Chinese Academy of Sciences, Shanghai, China) and cultured in Dulbecco's Modified Eagle Medium (DMEM, GibcoBRL, Gaithersburg, MD) supplemented with 10% fetal bovine serum (GibcoBRL, USA),100 U/ml of penicillin and 0.1 mg/ml of streptomycin in a humidified atmosphere at 5% CO_2 and 37 °C.

Recombinant adenoviral vectors expressing GRIM-19

The replication-deficient recombinant adenovirus expressing GRIM-19 was made using the AdEasy system. The human GRIM-19 cDNA (GenBank accession no. AF286697) was subcloned into pAdtrack-CMV from pIRES$_2$-EGFP/GRIM-19, resulting in pAdtrack-CMV/GRIM-19. The consensus Kozak sequence (CCACCATGG) was not introduced upstream of GRIM-19. All recombinant plasmids were verified by DNA sequencing (Sangon, Shanghai, China). The shuttle vector was used to generate recombinant Ad-GRIM-19 adenovirus as in a previously described method [20]. Large-scale viruses were propagated ($\leq$3) in 293T cells, purified by $CsCl_2$ gradient centrifugation and preserved in 0.01 M phosphate-buffered saline (PBS, pH 7.4). An adenovirus encoding GFP (Ad-GFP) was used as a control.

Flow cytometry (FCM) analysis

The percentage of GFP^+ cells was used to assess the efficiency of adenoviral transfer by flow cytometry (FCM) analysis. Subconfluent SGC-7901 cells were infected with Ad-GFP or Ad-GRIM-19 at a multiplicity of infection (MOI) ranging from 10 to 50 for 24 h, and then GFP^+ cells were counted by FCM analysis (Beckman Coulter, Fullerton, CA).

Immunofluorescence and confocal imaging

SGC-7901 cells were grown on glass cover slips to ~60% confluency and then infected with Ad-GFP or Ad-GRIM-19 before fixation. After 48 h, cells were fixed with 3% paraformaldehyde (PFA) for 15 min and ice-cold absolute methanol for 5 min, and then they were treated with blocking buffer (1× PBS + 0.2% Triton X-100 + 3% BSA). GRIM-19 expression was detected with GRIM-19 antibody. Signals were visualized by rhodamine-conjugated goat anti-mouse secondary antibodies, and the nucleus was visualized by DAPI staining. Images were captured with a Zeiss LSM-410 laser scanning microscopy (Zeiss, Oberkochen, Germany).

Trypan blue dye exclusion assay and cell morphology analysis

To assess possible cytotoxicity, Ad-GRIM-19-infected cells were stained using the Typan Blue Staining Cell Viability Assay (Beyotime, Haimen, China). Trypan blue staining was evaluated under the microscope, and cells were counted using a hemocytometer. Cells that took up trypan blue were counted as dead cells. In addition, cell morphological images were recorded by fluorescence microscopy (Lecia, Oberkochen, Germany).

RNA extraction and quantitative RT-PCR

Total RNA was extracted using the RNeasy Mini Kit (Qiagen, CA, USA), and was followed by cDNA synthesis using the ReverTra Ace-

α-first strand cDNA synthesis system (Toyobo, Osaka, Japan). In some cases, cells were treated with SN50 at a concentration of 25 or 50 μg/ml for 24 h. For quantitative RT-PCR analyses, the ABI PRISM 7500 Sequence Detection System (Applied Biosystems, Foster City, CA) and SYBR Green PCR Master Mix (Toyobo, Japan) were used with specific primers as follows: GW112: 5′-AGCTCTTTCCCAGGTGTTGA-3′ (forward), 5′-AAGCGTTCCACTCTGTCCAC-3′ (reverse); β-actin: 5′-CCAACCGCGAGAAGATGA-3′ (forward), 5′-CCAGAGGCGTA-CAGGGATAG-3′ (reverse). Quantification was carried out by normalizing levels to the amount of total cDNA using the ubiquitously expressed β-actin as a standard. Fold changes in gene expression were determined using the "2−ddCT" method [21].

Cell adhesion assay

For the cell adhesion assay, a 100-μl cell suspension that contained 5×10^4 cells was added to a 96-well culture plate coated with Matrigel™ (BD Biosciences, San Jose, CA, USA). After respective incubation for 0.5, 1, 2 and 4 h, the wells were washed twice with PBS gently. The optical density (450 nm) was detected by the Cell-Counting Kit-8 (CCK-8) (Dojindo, Kumamoto, Japan) using the Microplate Reader (Tacan, Swaziland). Each assay was performed in triplicate and repeated twice.

In vitro migration and invasion assay

Cell invasion assays were performed with the QCM ECMatrix Cell Invasion Assay kit (24-well, 8 μm, Millipore, NY, USA). SGC-7901 cells were infected with Ad-GFP or Ad-GRIM-19 for 24 h, and 1×10^4 cells were seeded per chamber. After incubating for 24 h, non-invading cells (upper chamber) were gently removed by using a cotton-tipped swab and invading cells (lower chamber) were fixed using methanol and stained with 2% Giemsa solution. The invasive ability was determined by the number of penetrating cells under a microscope at 200× magnification for 10 random fields in each well.

The method of *in vitro* migration assay was similar to the invasion assay described above using a non-Matrigel-coated 24-well Boyden Chamber (8 μm, Millipore). A total of 2×10^3 cells were used, and the incubation time was 24 h. Triplicate assays were performed for each group of cells in invasion and migration assays, and the results are expressed as means ± SD.

Tail vein metastatic assay

The tail vein metastatic assay was performed as previously described [22,23]. All animal procedures were approved by the Care of Experimental Animals Committee of Chongqing Medical University. Each nude mouse was inoculated subcutaneously through the tail vein with 1.5×10^6 tumor cells (non-infected cells, Ad-GFP-infected cells or Ad-GRIM-19-infected cells) after detection by trypan blue staining. The mice were then monitored for overall health and total body weight. After 4.5 weeks, the mice were sacrificed. The liver lobes were observed with the naked eye and the number of visible tumors on the liver surface was counted. Each group contained eight mice.

Preparation of nuclear and total extract

Nuclear and total extracts were prepared using NE-PER Nuclear and Cytoplasmic Extraction Reagents (Pierce, Rockford, USA) and RIPA buffer (Pierce), respectively. A quantity of 5×10^6 cells were infected for 72 h with the Ad-GFP or Ad-GRIM-19 adenovirus. Cells were washed two times with ice-cold PBS buffer and then subjected to nuclear and total extracts according to the protocol. Protein concentrations were determined using the BCA Protein assay kit (Pierce, Rockford, IL, USA), frozen in liquid nitrogen and stored at −80 °C until ready for analysis.

Electrophoretic mobility shift assay (EMSA)

The electrophoretic mobility shift assay (EMSA) was performed to assess NF-κB or STAT3 binding activity using a Light Shift chemiluminescent EMSA kit (Pierce, Rockford, Illinois, USA) according to the protocol. Briefly, 10 μg of nuclear extract was incubated with 0.5 μg each of poly (dIdC) in the presence of 20 fmol biotin-labeled wild-type (WT) or mutant double-stranded probe (Invitrogen, Shanghai, China) for 15 min at room temperature in a total volume of 20 μl. The probe consensus sequence (sense) was as follows: WT NF-κB: 5′-AGTTGAGGGGACTTTCCC-AGGC-3′; Mutant NF-κB: 5′-AGTTGAGGCGACTTTCCCAGGC-3′ (underlining indicates the mutant site). WT STAT3: 5′-GATCCTTCTGGGAATTCCTAGATC-3′; Mutant STAT3: 5′-GATCCTTCTGGGCCGTCCTAGATC-3′ (underlining indicates the mutant sites). EMSA competition experiments were performed in the presence of 50-fold excess of unlabeled NF-κB probe. DNA complexes were resolved from free probe with 4% non-denaturing polyacrylamide gels in 0.5× TBE buffer (pH 8.3) and detected by an enhanced chemiluminescence (ECL).

Western blot analysis

Western blots were performed to detect the expression of GW112, u-PA, MMP-2 and MMP-9. NF-κB p65/RelA and STAT3 in nuclear extracts were also analyzed. Culture supernatants were collected and concentrated approximately 20-fold using a spin-concentrator (Millipore, Bedford, MA). In some cases, cells were treated with SN50 at a concentration of 25 or 50 μg/ml for 24 h [22]. Proteins from both cell supernatants and lysates were measured using the BCA method. The same amount of protein was loaded in each lane, separated by 10–15% SDS-PAGE and then transferred to polyvinylidene difluoride (PVDF) membranes. The membranes were blocked with 5% nonfat milk, and then the membrane-bound proteins were probed with the above-mentioned primary antibodies followed by secondary horseradish peroxidase-conjugated antibodies. Protein bands were visualized by a supersignal chemiluminescence detection (ECL) kit (Pierce, Rockford, Illinois, USA).

Enzyme-linked immunospecific assay (ELISA)

SGC-7901 cells grown in 24-well plates were infected with Ad-GRIM-19 or Ad-GFP for 72 h. Protein levels of VEGF in the cell supernatant were determined by ELISA (R&D Systems). Samples were measured in triplicate and were properly diluted to ensure that measured values were within the concentration range of the standard curve.

Statistical analysis

Data from independent experiments were expressed as the mean ± S.D. of at least three experiments. Comparisons between groups were analyzed by two-tailed Student's *t*-test or ANOVA, as

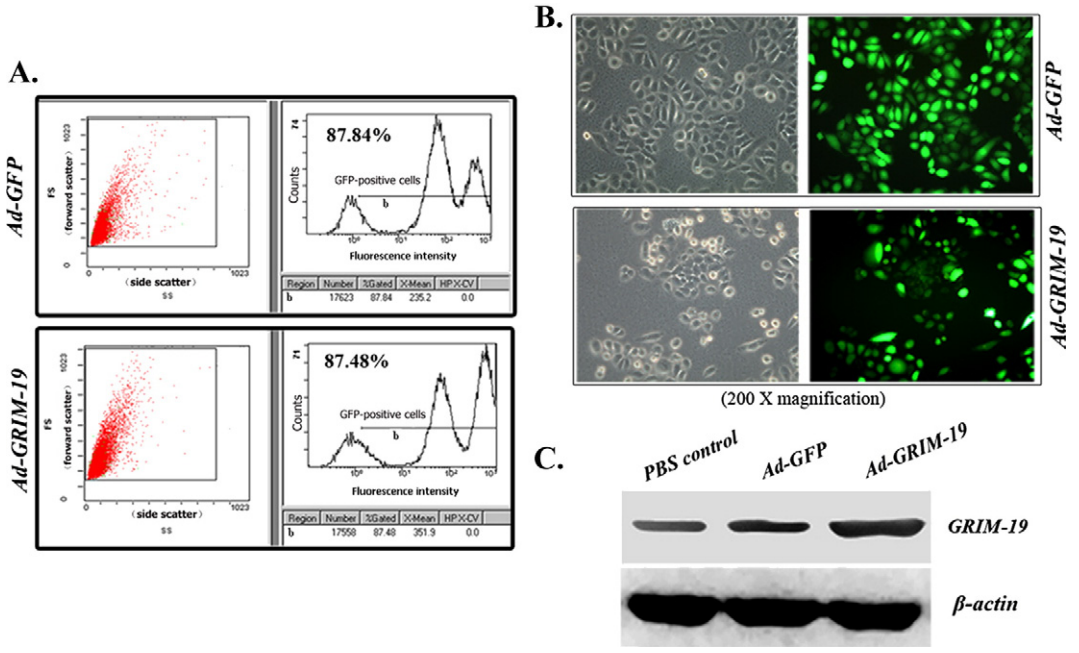

Fig. 1 – Efficient gene transduction and low cytotoxicity of Ad-GRIM-19 toward SGC-7901 cells. A. Flow cytometry (FCM) analysis was used to assess the efficiency of adenovirus. SGC-7901 cells were infected with adenovirus Ad-GFP or Ad-GRIM-19 for 24 h, the GFP+ cells were counted by FCM. Representatives of three experiments are shown. Left panel shows a one-colour dot plot of GFP+ cells. In the right panel (histogram plot of GFP+ cells), numbers show the percentage of GFP^+ cells and lowercase letter "b" presents the region of GFP+ cells. B. Images analysis was used to assess the effect of adenovirus infection on the cell morphology of SGC-7901 cells. Cells were infected with Ad-GFP or Ad-GRIM-19 for 48 h, and cell morphology was photographed with the use of an inverted fluorescence microscope (magnification, ×200). Representative images of three experiments are shown. C. Western blot for GRIM-19 proteins. Western blotting was performed using cell lysates following infection with Ad-GFP, Ad-GRIM-19 and PBS control at a MOI of 20 for 48 h with the gene-specific antibody as described in (A). Representatives of three experiments are shown.

appropriate, and p values <0.05 were considered to be statistically significant.

Results

Efficient gene transduction and low cytotoxicity of Ad-GRIM-19 toward SGC-7901 cells

After transduction with Ad-GFP or Ad-GRIM-19, GFP^+ SGC-7901 cells were measured by flow cytometry (FCM) analysis. As depicted in Fig. 1A, the percentages of GFP^+ SGC-7901 cells for Ad-GFP and Ad-GRIM-19 were 87.48% and 87.84%, respectively, at an MOI of 20. In addition, we assessed the possible cytotoxicity of Ad-GRIM-19 toward SGC-7901 cells with trypan blue staining cell viability assays and detected cell morphological changes. Fig. 1B shows that no apparent cell morphological changes with approximately 90% efficiency of Ad-GRIM-19-infected cells compared with the Ad-GFP group. Similar results were obtained from cell viability assays by trypan blue staining (data not shown). Moreover, infection of Ad-GRIM-19 notably increased GRIM-19 protein levels in SGC-7901 cells compared to Ad-GFP-infected cells and PBS controls (Fig. 1C and supplementary Fig. 1). Based on these results, we selected an MOI of 20 for infection of Ad-GRIM-19 to achieve highly efficient infection and low cytotoxicity toward SGC-7901 cells.

Upregulation of GRIM-19 inhibits GW112 expression

Previous studies have shown that the upregulation of some apoptosis-related genes induced by GRIM-19 was reversed by increased GW112, suggesting that these two molecules may potentially be involved in a common regulatory pathway. Therefore, we examined the effects of upregulated GRIM-19 on GW112 expression in gastric cancer cells. As shown in Fig. 2A, increased GRIM-19 in SGC-7901 cells (at a MOI of 20) resulted in a notable decrease of GW112 mRNA with a maximum of 85.6% decrease at 72 h after infection (Fig. 2A). In contrast, Ad-GFP control did not significantly affect GW112 or β-actin mRNA levels. Similar results were confirmed by western blotting (Fig. 2C).

GRIM-19 decreases NF-κB binding activity

Transcription factor NF-κB can bind to the GW112 promoter region and regulate GW112 expression. We therefore sought to determine whether NF-κB activation in SGC-7901 cells was involved in the downregulation of GW112 by GRIM-19. To investigate this possibility, nuclear extracts were mixed with either unlabeled probe sequence or with the biotin-labeled probe, and NF-κB binding activity was measured by EMSA. As shown in Fig. 3A (a), constitutive NF-κB binding activity was present in SGC-7901 cells, and the results revealed that Ad-GRIM-19-infected SGC-7901 cells exhibited

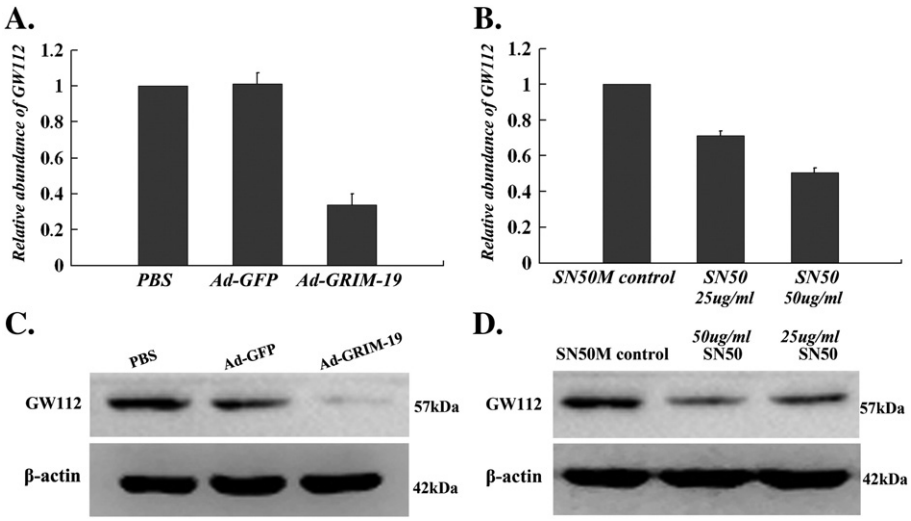

Fig. 2 – Infection of Ad-GRIM-19 or treatment with SN50 downregulates GW112 expression in SGC-7901 cells. SGC-7901 cells were treated with adenovirus (Ad-GFP or Ad-GRIM-19) or the NF-κB inhibitor SN50, and were then subjected to real-time PCR or western blot analysis, respectively. PBS-treated cells were used as a control. A. SGC-7901 cells were infected with Ad-GFP or Ad-GRIM-19 adenovirus. RNA was isolated and reverse-transcribed at 72 h post-infection. The relative abundance of GW112 mRNA was determined by real-time PCR using the "2-ddCT" method. β-actin was used as a standard control. Results represent the mean of three independent experiments performed in triplicate. B. SGC-7901 cells were treated with 25 or 50 μg/ml SN50 alone for 48 h. The relative abundance of GW112 mRNA was determined as described in (A). C and D. Western blot for GW112 protein. SGC-7901 cells were treated with adenovirus or SN50 as described in (A) and (B). The expression of GW112 protein was evaluated by western blotting. β-actin was used as an internal control. A representative of three experiments showing similar results is shown.

obviously decreased NF-κB binding activity compared with Ad-GFP-infected cells. GRIM-19 was reported to not interfere with the DNA binding activity of STAT3 although it has been shown to bind to STAT3 and inhibit its transcriptional activity [7,8]. We next examined the same nuclear extracts for STAT3 DNA binding activity. As expected in Fig. 3A (b), no obvious changes for the STAT3 binding activity were seen in the Ad-GRIM-19, Ad-GFP or PBS groups. As seen in Fig. 3A, These bindings could be completely eliminated by adding a 50-fold excess of unlabeled NF-κB or STAT3 oligonucleotide to the reaction mixture, although a small amount of nonspecific binding was shown in labeled mutant NF-κB or STAT3 probe lanes, confirming that the EMSA band was specific for NF-κB or STAT3 binding. It has been shown that GW112 expression can be regulated by the NF-κB p65/RelA subunit. p65/RelA and STAT3 protein levels were further detected in nuclear extracts. As seen in Fig. 3B, compared with PBS and Ad-GFP groups, p65/RelA level was reduced but STAT3 protein was not changed in Ad-GRIM-19-infected cells, which is accordance with EMSA results. These findings indicate that GRIM-19 has a pronounced regulatory capacity for NF-κB activation in highly metastatic SGC-7901 cells.

To further test whether NF-κB activation could regulate GW112 expression, SGC-7901 cells were treated with the specific NF-κB inhibitor SN50 or SN50M control. At 25 μg/ml or 50 μg/ml concentrations of SN50, we observed significantly decreased GW112 expression relative to SN50M controls (Figs. 2 B and D), supporting the conclusion that NF-κB can regulate GW112 expression.

Ad-GRIM-19 infection inhibits tumor cell adhesion, migration and invasion

Since NF-κB plays an important role in the adhesion, invasion and metastasis of gastric cancer cells, decreased NF-κB binding activity may exert direct effects on the biological behavior of SGC-7901 cells. To evaluate the effect of GRIM-19 on cell adhesion, the ability of SGC-7901 to adhere to Matrigel was investigated by an adhesion assay. All of the gastric cancer cells bound to Matrigel in a time-dependent manner. As depicted in Fig. 4A, the upregulation of exogenous GRIM-19 significantly decreased the cells' abilities to adhere to Matrigel at 2 h and 4 h. ($p<0.05$).

Cell migration and invasion are critical processes in tumor metastasis. We investigated the effects of GRIM-19 on SGC-7901 cell migration by non-Matrigel-coated Boyden chamber or cell invasion by Matrigel-coated invasion chamber assays, respectively. In the *in vitro* migration assays (Fig. 4B), the average migratory cell number of the SGC-7901 cells was significantly decreased compared to that of the control cells ($p<0.05$). As shown in Fig. 4C, Ad-GRIM-19 infection produced notable inhibition of the invasive ability of SGC-7901 cells through Matrigel in a Boyden chamber assay, with an average inhibitory rate of approximately 39.5% compared with the Ad-GFP control ($p<0.01$).

Inhibitory effect of GRIM-19 on liver metastasis in SGC-7901 cells

To examine the *in vivo* metastatic ability of Ad-GRIM-19-infected SGC-7901 cells, we performed tail vein metastatic assays in nude mice. After infection for 24 h, SGC-7901 cells were injected into mice through the tail vein. Compared with control cells infected with Ad-GFP or PBS, intravenous inoculation of SGC-7901 cells led to significantly fewer visible metastases on the liver surface ($p<0.01$) (Fig. 4D). In addition, the metastases (with diameters approx. 0.8–1.3 mm) deprived from cells treated with Ad-GRIM-19 were smaller than those in controls (with diameters approx. 1–2 mm) (data not shown).

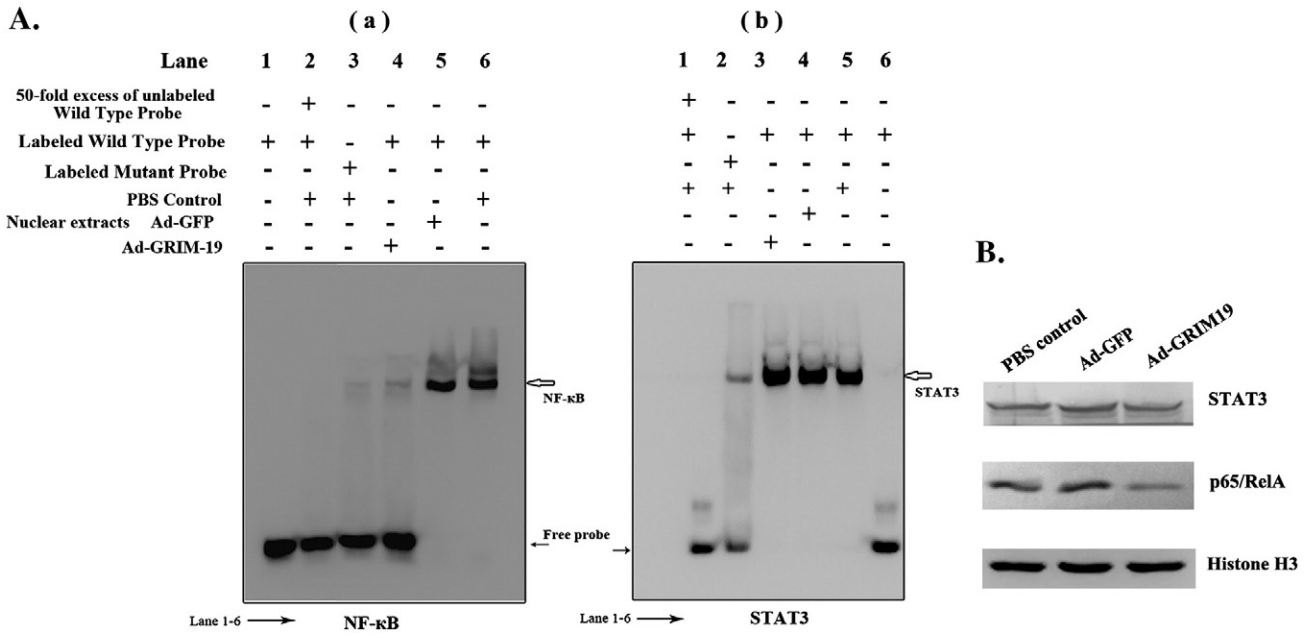

Fig. 3 – Infection of Ad-GRIM-19 represses NF-κB binding activity and reduces p65/RelA expression in nuclear extracts of SGC-7901 cells. Cells were infected with Ad-GFP or Ad-GRIM-19 for 72 h. Nuclear extracts were isolated and subjected to electrophoretic mobility shift assay (EMSA) for NF-κB or STAT3 binding activity and to western blotting for NF-κB p65/RelA and STAT3 expressions respectively. A. EMSA for NF-κB or STAT3 binding activity. An equal amount (10 μg) of nuclear protein was loaded and analysis was performed by using the binding reactions. After reactions, samples were run on 4% non-denaturing polyacrylamide gels and analyzed by enhanced chemiluminescence (ECL). A representative of three experiments is shown. (a) EMSA for NF-κB binding activity. Lane 1: biotin-labeled WT (wild-type) NF-κB probe; Lane 2: 50× excess of unlabeled WT NF-κB probe + labeled WT NF-κB probe + nuclear extracts (PBS control); Lane 3:labeled mutant NF-κB probe + nuclear extracts (PBS control); Lane 4: labeled WT NF-κB probe + nuclear extracts (Ad-GRIM-19 group); Lane 5: labeled WT NF-κB probe + nuclear extracts (Ad-GFP group); Lane 6: labeled WT NF-κB probe + nuclear extracts (PBS control). (b) EMSA for STAT3 binding activity. Lane 1: 50× excess of unlabeled WT STAT3 probe + labeled WT STAT3 probe + nuclear extracts (PBS control); Lane 2: labeled mutant STAT3 probe + nuclear extracts (PBS control); Lane 3: labeled WT STAT3 probe + nuclear extracts (Ad-GRIM-19 group); Lane 4: labeled WT STAT3 probe + nuclear extracts (Ad-GFP group); Lane 5: labeled WT STAT3 probe + nuclear extracts (PBS control); Lane 6: labeled WT STAT3 probe. B. Western blot for NF-κB p65/RelA and STAT3 expression in nuclear extracts. An equal amount (30 μg) of nuclear extracts was loaded and separated by 10–15% SDS-PAGE. After transferring to PVDF membranes, NF-κB p65/RelA and STAT3 expressions levels were detected with primary antibodies. Histone H3 was used as an internal control. A representative of three experiments is shown.

MMP-2, MMP-9, VEGF and u-PA are involved in the invasion of gastric cancer regulated by GRIM-19

Our finding that GRIM-19 had an inhibitory effect on invasion prompted us to examine its effects on the expression of u-PA, MMP-2, MMP-9 and VEGF in gastric cancer cells. As depicted in Fig. 5A, ELISA analysis revealed that VEGF excretion in the supernatant from Ad-GRIM-19-infected cells was significantly decreased ($p<0.05$), while no obvious changes were observed in the Ad-GFP and PBS groups. Western blot analysis displayed an obvious decrease in MMP-2, MMP-9 and u-PA proteins in the supernatant and in total extracts from Ad-GRIM-19 infected SGC-7901 cells compared to the Ad-GFP and PBS groups (Fig. 5B). The results were reproducible in at least three independent batches of experiments. Taken together, these results suggest that the inhibitory effect of GRIM-19 on metastasis of gastric cancer was at least partially mediated by the downregulation of u-PA, MMP-9, MMP-2 and VEGF, which may contribute to degradation of the extracellular matrix.

Discussion

Gastric cancer is one of the most common malignancies in the world, particularly in Eastern Asian countries such as China, Korea, and Japan [24], and it is characterized by its high capacity for invasion and metastasis [25]. Metastasis is a mortal factor for gastric cancer patients. Currently, the mechanisms by which gastric cancer metastasize are not fully understood. Our results demonstrate that GRIM-19 can inhibit the invasive and metastatic abilities of gastric cancer cells. The observed inhibitory effect of GRIM-19 was at least partially mediated by the NF-κB pathway and, as a consequence, decreased secretions of MMP-9, VEGF, u-PA and MMP-2.

GRIM-19, originally described as a suppressor of cell growth in response to IFN-retinoid treatment, has been shown to enhance the sensitivity of cells to IFN/RA-induced death [3,4]. Although introduction of the GRIM-19 gene into cancer cells by plasmid vectors has been reported previously [7,8,10], including in therapeutic trials [26], a low transduction efficiency and transient

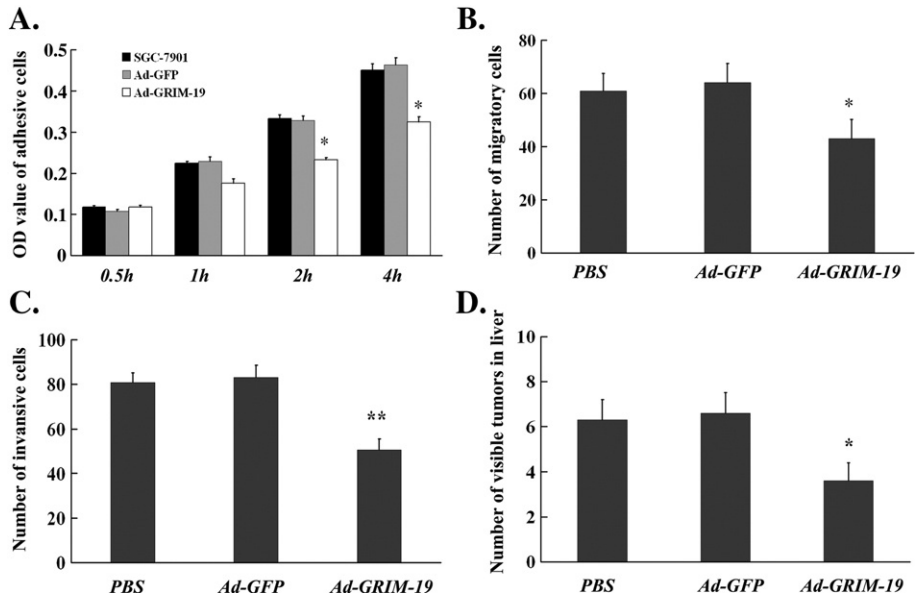

Fig. 4 – Effects of upregulation of GRIM-19 on the adhesive, invasive, migratory and metastatic abilities of SGC-7901 cells. Cells were infected with Ad-GFP, Ad-GRIM-19 or PBS control for 24 h, and then were subjected to the following experiments. A representative of three experiments with similar results is shown. A. Cell adhesion assay. After 0.5, 1, 2 and 4 h of incubation, the cells attached to Matrigel were assessed for OD value using the CCK-8 assay kit. Results are expressed as the mean ± S.D. of three independent experiments performed in triplicate. *: $p < 0.05$ compared with the control. B. In vitro migration assay. Migration of SGC-7901 cells was analyzed using a non-Matrigel-coated Boyden chamber (8 μm). The migration ability was determined by the number of migrated cells under a microscope at 200× magnification for 10 random fields in each well. Data is expressed as the mean ± S.D. of three experiments *: $p < 0.05$ compared with the control. C. In vitro invasion assay. Invasive ability was evaluated by counting cells invading through Matrigel and a membrane in a Matrigel-coated invasiveness chamber (8 μm).The number of penetrating cells was counted a microscope at 200× magnification for 10 random fields in each well. Data are mean ± S.D. of three experiments **: $p < 0.01$ compared with the PBS control. D. Nude mice were injected with 1.5×10^6 cells through tail veins. Experimental and control groups had eight mice each. At 4.5 weeks later, the mice were sacrificed. The liver lobes were observed by the naked eye, and the number of visible tumors on the liver surfaces was counted. Data are mean ± S.D. **: $p < 0.01$ versus cells infected with Ad-GFP *: $p < 0.05$ versus control cells.

expression by the plasmid-based approach limits its application in clinical therapy. Recently, an adenovirus-based approach has been shown to have many advantages over plasmid vectors, including a broad range of infectivity, high titers, high transduction efficiencies and safety. This approach has become a versatile tool for gene delivery in clinical trials to treat cancer by means of gene therapy [27]. Given the results presented here, we believe that adenovirus-mediated GRIM-19 transfer would be a promising candidate for a similar gene therapy treatment. However, constructing GRIM-19 adenovirus with the Adeasy system is very difficult due to the potential toxicity of overexpressed GRIM-19 to host cells [10]. Some studies have reported that the overexpression of GRIM-19 in some cell types causes cell death, at the same time they also showed that the same cancer cells could also be stably transfected by moderately expressed GRIM-19 to slow cell growth rather than induce cell death [8]. In our unpublished data, a consensus Kozak sequence-mediated GRIM-19 "superexpression" induced notable cell death of SGC-7901 cells by mitochondrial aggregation and nuclear damage. These findings indicate that different degrees of exogenous GRIM-19 expression may differentially affect cancer cells.

In the present study, we successfully constructed an adenoviral vector expressing human GRIM-19 that displayed highly efficient gene transduction and low cytotoxicity in SGC-7901 cells. Using Ad-GRIM-19, we found that enhanced GRIM-19 resulted in a down-regulation of GW112 expression. GW112, which is frequently overexpressed in gastric cancers, is notable for its ability to reverse the induction of apoptotic genes by GRIM-19, indicating a potential interaction between GRIM-19 and GW112. Initially, we explored the effect of overexpression or knockdown of GW112 on GRIM-19. However, the GRIM-19 expression seems to be unaffected by these perturbations, indicating that GW112 might be downstream of GRIM-19 (data not shown). Our efforts to knockdown endogenous GRIM-19 by small-interfering RNA (siRNA) and assess its effect on GW112 expression failed because of the unexpected cell death in GRIM-19-siRNA-transfected SGC-7901 cells (data not shown). We speculate that GRIM-19, which is a crucial subunit for the assembly and function of mitochondrial complex I [28,29], is essential for the survival of SGC-7901 cells. We then constructed Ad-GRIM-19 adenovirus and transduced it into SGC-7901 cells. As expected, the exogenously enhanced GRIM-19 downregulated GW112 expression, indicating that GRIM-19 is an upstream regulator of GW112.

It is not known which signaling intermediates downstream of GRIM-19 regulate the expression of GW112 in gastric cancer. Several recent studies have emerged concerning the mechanism of GW112 regulation by GRIM-19. In pancreatic cancer PANC-1 cells and myeloid precursor cells, treatment with the specific PI3K-inhibitor LY294002 decreased GW112 levels, implicating the PI3K/Akt pathway in the regulation of GW112 expression [18,30]. Furthermore, the transcription factor NF-κB, a substrate of Akt [31–33], has been shown to directly activate GW112 at the transcriptional level

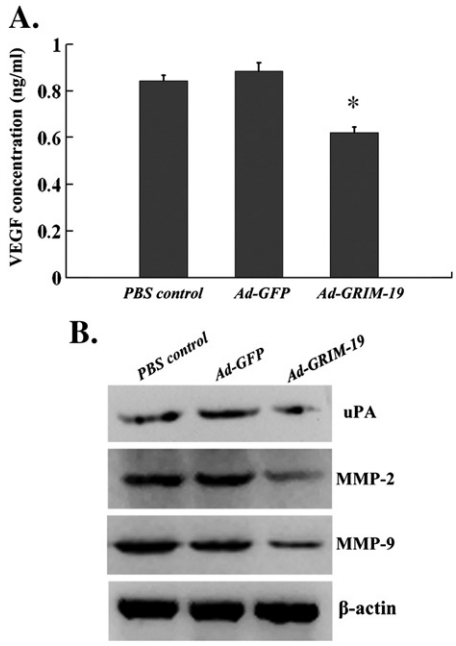

Fig. 5 – The effect of GRIM-19 on MMP-9, VEGF, u-PA and MMP-2 expression in SGC-7901 cells. A. The concentration of VEGF was evaluated by ELISA. Supernatants from SGC-7901 cells infected with Ad-GFP, Ad-GRIM-19 or PBS control were subjected to ELISA analysis. The results represented are the mean of three independent experiments performed in triplicate and are expressed as the mean ± S.D. *: $p < 0.05$ compared to the control. B. Western blot analysis was used to assess expressions of u-PA, MMP-2 and MMP-9 using antibodies against u-PA, MMP-2 and MMP-9. β-actin was used as an internal control. A representative of three experiments is shown.

by binding to specific sites in the 5′-proximal promoter region [30]. Given these findings, we hypothesize that NF-κB activation might be involved in the regulation of GRIM-19 to GW112. Here, we showed that NF-κB binding activity was blocked by the upregulation of GRIM-19. We also observed that GW112 expression was down-regulated upon treatment with a NF-κB inhibitor, SN50. As it has been reported that the forced overexpression of the NF-κB p65/RelA can induce GW112 expression [34], we further examined p65/RelA levels in nuclear extracts by western blotting and showed that p65/RelA levels were reduced in nuclear extracts. These results strongly indicate that decreased NF-κB activity and reduced p65/RelA levels are responsible for the suppression of GW112 expression by GRIM-19 in SGC-7901 cells. We therefore propose that NF-κB signaling maybe as a functional link between GRIM-19 and GW112. The underlying mechanisms accounting for the regulation of the NF-κB signal by GRIM-19 will be the subject of further investigation.

Our study observed that the infection of Ad-GRIM-19 in SGC-7901 cells suppressed cells' adhesive, migratory, invasive and liver metastatic abilities and decreased the release of growth factors or chemokines such as VEGF, MMP-2, MMP-9 and u-PA. NF-κB is an important factor during cancer cell invasion and metastasis [22,35–37,39], and its constitutive activation has been found in gastric carcinoma [33,35,37] and gastric cancer SGC-7901 cell line [22,37]. Blocking NF-κB strongly suppresses SGC-7901 cell migration and invasion in both *in vitro* and *in vivo* metastasis [22], suggesting that NF-κB activation plays an important role in metastatic processes in gastric cancer. The gastric cancer SGC-7901 cell line was shown to have the invasive ability to penetrate Matrigel-coated Boyden Chamber plates in an invasion assay *in vitro* and to metastasize mainly to the liver rather than the lung and other organs in a tail vein metastatic assay *in vivo* [22,23]. We found that the upregulation of GRIM-19 inhibited the invasion and metastasis of gastric cancer both in an *in vitro* invasion assay and in an *in vivo* tail vein metastatic assay. GRIM-19 has been also shown to inhibit src-induced cell motility and metastasis by suppressing the tyrosyl phosphorylation of focal adhesion kinase (FAK), paxillin, E-cadherin and γ-catenin [9]. Based on the above findings, therefore, it is conceivable that GRIM-19 has the potential to suppress cancer cells' adhesive, invasive, migratory and metastatic abilities.

Extracellular matrix degradation is an essential step in tumor invasion and metastasis, and it is mainly mediated by the secretion of MMP-2 [38], MMP-9 [22,40,41] and VEGF [42,43], as well as the serine protease u-PA protein [22,44,45]. Numerous studies of NF-κB-regulated MMP-9, u-PA and VEGF levels have been shown to affect cancer behaviors such as adhesion and invasion [43–46]. In SGC-7901 cells, the inhibition of NF-κB activation by SN50 inhibits the expression of u-PA and MMP-9, and treatment with u-PA or MMP-9 antibody can inhibit the invasive ability of SGC-7901 cells [22]. In addition, the blockade of NF-κB activity has been shown to downregulate VEGF expression and suppress metastasis in a number of cancer cell lines [46], suggesting that u-PA, MMP-9 and VEGF play important roles in metastasis in gastric cancer. In our study, the expression of these proteins was downregulated in Ad-GRIM-19-infected cells.

However, we cannot exclude other signaling intermediates outside of the NF-κB pathway that could be responsible for the GRIM-19-mediated inhibition of invasion and metastasis of gastric cancer cells in this study. To date, aberrantly active STAT3, which has been shown to promote tumor cell growth and survival via a continual induction of pro-growth genes such as VEGF [40,41,46] and MMP-2 [26,39], was also detected in gastric cancer SGC-7901 cells [47]. Blockade of constitutive STAT3 activity in gastric cancer cells inhibited cell invasion and metastasis and suppressed the expression of VEGF and MMP-2 [46]. Our finding that MMP-2 was decreased in Ad-GRIM-19-infected SGC-7901 cells is in accordance with a recent observation that treatment with GRIM-19 plasmids suppressed MMP-2 activity in a highly invasive PC-3 M prostate tumor model [26]. However, it seems to conflict with a study in which the inhibition of NF-κB could not affect MMP-2 expression in SGC-7901 cells [22]. GRIM-19, functioning as a negative regulator of STAT3, could inhibit the STAT3-driven expression of VEGF and MMP-2. The most plausible explanation is that the downregulation of MMP-2 levels by Ad-GRIM-19 is associated with the inhibition of STAT3 transcriptional activation rather than NF-κB inactivation. Therefore, interplay between GRIM-19 and other signaling intermediates is likely involved and remains to be more extensively investigated in future studies.

In addition, we also noticed that GRIM-19 downregulated GW112 expression in gastric cancer SGC-7901 cells. However, in presently, the exact function of GW112 has yet to completely elucidated. Even though GW112 has been shown to facilitate cell adhesion in NIH3T3 and HEK293 cells and promote cell proliferation in prostate cancer, and to be correlative with invasion and metastasis [12,15–18], whereas the adhesion and migration suppression effects and unchanged cell proliferation were observed in GW112-over-expressing colon carcinoma HT-29 cells [48]. These controversial

observations suggest that cell-specific effects maybe exist for the GW112 gene. Further systematic investigations are necessary to clarify the role of deregulated GW112 in gastric cancer.

In conclusion, the present study provides evidence that Ad-GRIM-19 infection results in decreased GW112 and suppressed tumor adhesion, *in vitro* invasion and *in vivo* metastasis of metastatic human gastric cancer cells. The inhibition of tumor invasion and abrogation of metastasis by Ad-GRIM-19 is correlated with decreased MMP-2, MMP-9, VEGF and u-PA, and is at least partially mediated by the downregulation of NF-κB binding activation. Collectively, these data suggest that the adenovirus-mediated transfer of the GRIM-19 gene may be a potential approach to controlling the invasion and metastasis of human gastric cancer.

Acknowledgments

This work was supported by grants from the National Nature Science Foundation of China (no. 30701004). Appreciation goes to Dr. Kebin Zhang and Lixia Guang for their encouragement and kind help in this work.

Appendix A Supplementary data

Supplementary data associated with this article can be found, in the online version, at doi:10.1016/j.yexcr.2010.05.010.

REFERENCES

[1] D.J. Lindner, E.C. Borden, D.V. Kalvakolanu, Synergistic antitumor effects of a combination of interferons and retinoic acid on human tumor cells in vitro and in vivo, Clin. Cancer Res. 3 (1997) 931–937.
[2] D.M. Moore, D.V. Kalvakolanu, S.M. Lippman, J.J. Kavanagh, W.K. Hong, E.C. Borden, M. Paredes-Espinoza, I.H. Krakoff, Retinoic acid and interferon in human cancer: mechanistic and clinical studies, Semin. Hematol. 31 (1994) 31–37.
[3] J.E. Angell, D.J. Lindner, P.S. Shapiro, E.R. Hofmann, D.V. Kalvakolanu, Identification of GRIM-19, a novel cell death-regulatory gene induced by the interferon-β and retinoic acid combination, using a genetic approach, J. Biol. Chem. 275 (2000) 33416–33426.
[4] G. Huang, Y. Chen, H. Lu, X. Cao, Coupling mitochondrial respiratory chain to cell death: an essential role of mitochondrial complex I in the interferon-beta and retinoic acid-induced cancer cell death, Cell Death Differ. 14 (2007) 327–337.
[5] I. Alchanati, S.C. Nallar, P. Sun, L. Gao, J. Hu, A. Stein, E. Yakirevich, D. Konforty, I. Alroy, X. Zhao, S.P. Reddy, M.B. Resnick, D.V. Kalvakolanu, A proteomic analysis reveals the loss of expression of the cell death regulatory gene GRIM-19 in human renal cell carcinomas, Oncogene 25 (2006) 7138–7147.
[6] N.V. Chidambaram, J.E. Angell, W. Ling, E.R. Hofmann, D.V. Kalvakolanu, Chromosomal localization of human GRIM-19, a novel IFN-β and retinoic acid- activated regulator of cell death, J. Interferon Cytokine Res. 20 (2000) 661–665.
[7] C.C. Lufei, J. Ma, G. Huang, T. Zhang, V. Novotny-Diermayr, C.T. Ong, X.M. Cao, GRIM-19, a death regulatory gene product, suppresses Stat3 activity via functional interaction, EMBO J. 22 (2003) 1325–1335.
[8] J. Zhang, J. Yang, S.K. Roy, S. Tininini, J. Hu, J.F. Bromberg, V. Poli, G. R. Stark, D.V. Kalvakolanu, The cell death regulator GRIM-19 is an inhibitor of signal transducer and activator of transcription 3, Proc. Natl. Acad. Sci. U. S. A. 100 (2003) 9342–9347.
[9] S. Kalakonda, S.C. Nallar, P. Gong, D.J. Lindner, S.E. Goldblum, S.P. Reddy, D.V. Kalvakolanu, Tumor suppressive protein gene associated with retinoid-interferon-induced mortality (GRIM)-19 inhibits src-induced oncogenic transformation at multiple levels, Am. J. Pathol. 171 (2007) 1352–1368.
[10] T. Seo, D. Lee, Y.S. Shim, J.E. Angell, N.V. Chidambaram, D.V. Kalvakolanu, J. Choe, Viral interferon regulatory factor 1 of Kaposi's sarcoma associated herpesvirus interacts with a cell death regulator, GRIM19, and inhibits interferon/retinoic acid-induced cell death, J. Virol. 76 (2002) 8797–8807.
[11] X. Zhang, Q. Huang, Z. Yang, Y.P. Li, C.Y. Li, GW112, a novel antiapoptotic protein that promotes tumor growth, Cancer Res. 64 (2004) 2474–2481.
[12] W. Liu, L. Chen, J. Zhu, G.P. Rodgers, The glycoprotein hGC-1 binds to cadherin and lectins, Exp. Cell Res. 312 (2006) 1785–1797.
[13] J. Zhang, W.L. Liu, D.C. Tang, L. Chen, M. Wang, S.D. Pack, Z. Zhuang, G.P. Rodgers, Identification and characterization of a novel member of olfactomedin-related protein family, hGC-1, expressed during myeloid lineage development, Gene 283 (2002) 83–93.
[14] S. Koshida, D. Kobayashi, R. Moriai, N. Tsuji, N. Watanabe, Specific overexpression of OLFM4$^{GW112/hGC-1}$ mRNA in colon, breast and lung cancer tissues detected using quantitative analysis, Cancer Sci. 98 (2007) 315–320.
[15] W. Yasui, N. Oue, P.P. Aung, S. Matsumura, M. Shutoh, H. Nakayama, Molecular-pathological prognostic factors of gastric cancer: a review, Gastric Cancer 8 (2005) 86–94.
[16] P.P. Aung, N. Oue, Y. Mitani, H. Nakayama, K. Yoshida, T. Noguchi, A.K. Bosserhoff, W. Yasui, Systematic search for gastric cancer-specific genes based on SAGE data: melanoma inhibitory activity and matrix metaloproteinase-10 are novel prognostic factors in patients with gastric cancer, Oncogene 25 (2006) 2546–2557.
[17] W. Liu, J. Zhu, L. Cao, G.P. Rodgers, Expression of hGC-1 is correlated with differentiation of gastric carcinoma, Histopathology 51 (2007) 157–165.
[18] N. Oue, P.P. Aung, Y. Mitani, H. Kuniyasu, H. Nakayama, W. Yasui, Genes involved in invasion and metastasis of gastric cancer identified by array-based hybridization and serial analysis of gene expression, Oncology 69 (2005) 17–22.
[19] D. Kobayashi, S. Koshida, R. Moriai, N. Tsuji, N. Watanabe, Olfactomedin 4 promotes S-phase transition in proliferation of pancreatic cancer cells, Cancer Sci. 98 (2007) 334–340.
[20] T.C. He, S. Zhou, L.T. da Costa, J. Yu, K.W. Kinzler, B. Vogelstein, A simplified system for generating recombinant adenoviruses, Proc. Natl. Acad. Sci. U. S. A. 95 (1998) 2509–2514.
[21] K.J. Livak, T.D. Schmittgen, Analysis of relative gene expression data using real-time quantitative PCR and the $2-\Delta\Delta$ CT method, Methods 25 (2001) 402–408.
[22] H.F. Jin, Y.L. Pan, L.J. He, H.H. Zhai, X.H. Li, L.N. Zhao, L. Sun, J. Liu, L. Hong, J.G. Song, H.H. Xie, J.A. Gao, S. Han, Y. Li, D. Fan, p75 Neurotrophin receptor inhibits invasion and metastasis of gastric cancer, Mol. Cancer Res. 5 (2007) 423–433.
[23] Y. Pan, L. Zhao, J. Liang, J. Liu, Y. Shi, N. Liu, G. Zhang, H. Jin, J. Gao, H. Xie, J. Wang, Z. Liu, D. Fan, Cellular prion protein promotes invasion and metastasis of gastric cancer, FASEB J. 20 (2006) 1205–1215.
[24] S.R. Alberts, A. Cervantes, C.J. van de Velde, Gastric cancer: epidemiology, pathology and treatment, Ann. Oncol. 14 (2003) 31–36.
[25] E. Tahara, Molecular aspects of invasion and metastasis of stomach cancer, Verh. Dtsch Ges. Pathol. 84 (2000) 43–49.
[26] L. Zhang, L.F. Gao, Y. Li, G.M. Lin, Y.T. Shao, K. Ji, H. Yu, D.V. Kalvakolanu, D.J. Kopecko, X.J. Zhao, D.Q. Xu, J. Hu, Effects of plasmid-based Stat3-specific short hairpin RNA and GRIM-19 on PC-3M tumor cell growth, Clin. Cancer Res. 14 (2008) 559–568.
[27] K. Benihoud, P. Yeh, M. Perricaudet, Adenovirus vectors for gene delivery, Curr. Opin. Biotechnol. 10 (1999) 440–447.

[28] I.M. Fearnley, J. Carroll, R.J. Shannon, M.J. Runswick, J.E. Walker, J. Hirst, GRIM-19, a cell death regulatory gene product, is a subunit of bovine mitochondrial NADH: ubiquinone oxidoreductase (complex I), J. Biol. Chem. 276 (2001) 38345–38348.
[29] G. Huang, H. Lu, A. Hao, D.C. Ng, S. Ponniah, K. Guo, C.C. Lufei, Q. Zeng, X.M. Caoj, GRIM-19, a cell death regulatory protein, is essential for assembly and function of mitochondrial complex I, Mol. Cell. Biol. 24 (2004) 8447–8456.
[30] K.L. Chin, W. Aerbajinai, J. Zhu, L. Drew, L. Chen, W. Liu, G.P. Rodgers, The regulation of OLFM4 expression in myeloid precursor cells relies on NF-[kappa] B transcription factor, Br. J. Haematol. 143 (2008) 421–443.
[31] L.V. Madrid, C.Y. Wang, D.C. Guttridge, A.J. Schottelius, A.S. Jr Baldwin, M.W. Mayo, Akt suppresses apoptosis by stimulating the transactivation potential of the RelA/p65 subunit of NF-κB, Mol. Cell. Biol. 20 (2000) 1626–1638.
[32] A. Mansell, N. Khelef, P. Cossart, L.A. O'Neill, Internalin B activates nuclear factor-kB via Ras, phosphoinositide 3-kinase, and Akt, J. Biol. Chem. 276 (2001) 43597–43603.
[33] B.L. Lee, H.S. Lee, J. Jung, S.J. Cho, H.Y. Chung, W.H. Kim, Y.W. Jin, C. S. Kim, S.Y. Nam, Nuclear factor-kappaB activation correlates with better prognosis and Akt activation in human gastric cancer, Clin. Cancer Res. 7 (2005) 2518–2525.
[34] K.K. Kim, K.S. Park, S.B. Song, K.E. Kim, Up regulation of GW112 Gene by NFκB promotes an antiapoptotic property in gastric cancer cells, Mol. Carcinog. 49 (2010) 259–270.
[35] B. Rayet, C. Gélinas, Aberrant rel/nfkb genes and activity in human cancer, Oncogene 18 (1999) 6938–6947.
[36] G. Sethi, K.S. Ahn, B. Sung, B.B. Aggarwal, Pinitol targets nuclear factor-κB activation pathway leading to inhibition of gene products associated with proliferation, apoptosis, invasion, and angiogenesis, Mol. Cancer Ther. 7 (2008) 1604–1614.
[37] Q. Li, Y.Y. Yu, Z.G. Zhu, Y.B. Ji, Y. Zhang, B.Y. Liu, X.H. Chen, Y.Z. Lin, Effect of NF-kB constitutive activation on proliferation and apoptosis of gastric cancer cell lines, Eur. Surg. Res. 37 (2005) 105–110.
[38] H.L. Pahl, Activators and target genes of Rel/NF-κB transcription factors, Oncogene 18 (1999) 6853–6866.
[39] T.X. Xie, D.Y. Wei, M.G. Liu, A.C. Gao, F. Ali-Osman, R. Sawaya, S.Y. Huang, Stat3 activation regulates the expression of matrix metalloproteinase-2 and tumor invasion and metastasis Oncogene 23 (2004) 3550–3560.
[40] A.R. Farina, A. Tacconelli, A. Vacca, M. Maroder, A. Gulino, A.R. Mackay, Transcriptional up-regulation of matrix metallo proteinase-9 expression during spontaneous epithelial to neuroblast phenotype conversion by SK-N-SH neuroblastoma cells, involved in enhanced invasivity, depends upon GT-box and nuclear factor κB elements, Cell Growth Differ. 10 (1999) 353–367.
[41] M. Bond, R.P. Fabunmi, A.H. Baker, A.C. Newby, Synergistic upregulation of metalloproteinase-9 by growth factors and inflammatory cytokines: An absolute requirement for transcription factor NF-κB, FEBS Lett. 435 (1998) 29–34.
[42] G. Niu, K.L. Wright, M. Huang, L. Song, E. Haura, J. Turkson, S. Zhang, T. Wang, D. Sinibaldi, D. Coppola, R. Heller, L.M. Ellis, J. Karras, J. Bromberg, D. Pardoll, R. Jove, H. Yu, Constitutive Stat3 activity upregulates VEGF expression and tumor angiogenesis, Oncogene 21 (2002) 2000–2008.
[43] A.T. Hooper, G. Akiri, D. Jin, S.V. Shmelkov, E. Chuang, S.J. Shin, Y. Wu, D.J. Hicklin, S. Rafii, L.T. Vahdat, VEGF receptor expression on reactive breast cancer stroma: paving the way for tumor invasion, J. Clin. Oncol. 23 (2005) 9642–9650.
[44] J.Y. Cho, H.C. Chung, S.H. Noh, J.K. Roh, J.S. Min, B.S. Kim, High level of urokinase-type plasminogen activator is a new prognostic marker in patients with gastric carcinoma, Cancer 79 (1997) 878–883.
[45] T. Kaneko, H. Konno, M. Baba, T. Tanaka, S. Nakamura, Urokinase-type plasminogen activator expression correlates with tumor angiogenesis and poor outcome in gastric cancer, Cancer Sci. 94 (2003) 43–49.
[46] D.Y. Wei, X.D. Le, L.Z. Zheng, L.W. Wang, J.A. Frey, A.C. Gao, Z.H. Peng, S.Y. Huang, H.Q. Xiong, J.L. Abbruzzese, K.P. Xie, Stat3 activation regulates the expression of vascular endothelial growth factor and human pancreatic cancer angiogenesis and metastasis, Oncogene 22 (2003) 319–329.
[47] L.F. Yu, Y.B. Zhu, M.M. Qiao, J. Zhong, S.P. Tu, Y.L. Wu, Constitutive activation and clinical significance of Stat3 in human gastric cancer tissues and cell lines, Zhong Hua Yi Xue Za Zhi 84 (2004) 2064–2069.
[48] W. Liu, Y. Liu, J. Zhu, E. Wright, I. Ding, G.P. Rodgers, Reduced hGC-1 protein expression is associated with malignant progression of colon carcinoma, Clin. Cancer Res. 14 (2008) 1041–1049.